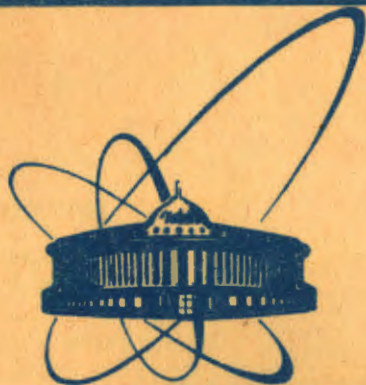


82-472



сообщения
объединенного
института
ядерных
исследований
Дубна

Экз. чит. зала

E1-82-472

**A.M.Baldin, V.K.Bondarev, N.Ghiordanescu,
A.N.Khrenov, A.G.Litvinenko, A.N.Manyatovsky,
N.S.Moroz, Yu.A.Panebratsev, M.Pentia,
S.V.Rikhvitsky, V.S.Stavinsky**

**EXPERIMENTAL DATA
ON INCLUSIVE CROSS SECTION
FOR CUMULATIVE PRODUCTION
OF PIONS, KAONS, ANTIPROTONS
AND THE QUARK-PARTON STRUCTURE
FUNCTION OF NUCLEI**

1982

INTRODUCTION

Nuclear reactions with large momentum transfers at relativistic energies are of much interest due to the fact that according to the existing ideas they must essentially be affected by quark structure of atomic nuclei. The study of nuclear quark structure is certain to give new information about multi-quark systems and interactions, which is important for the construction of large-distance quantum chromodynamics (QCD). Cumulative production of particles, that is, production of particles beyond the kinematic limits of one-nucleon collisions, is in this connection of a special interest and is the subject of many experimental and theoretical papers (see, e.g. reviews^{/1,2,3/}). The notion of cumulative effect has originated from the ideas that the hadron interaction at large momentum transfers is local and that a point-like object perceiving a momentum larger than that of the whole nucleon belongs to the group of nucleons of the nucleus^{/5/}. It is just in this sense that we mean cumulation^{/6/}. The point-like character of interactions of hadrons possessing internal structure (dynamically deformable form factor) was first postulated by Markov as long before as the quark hypothesis was suggested. He had made the important prediction that the total lepton-nucleon interaction cross sections tend, as the energy increases, to the elastic point-like particle cross sections. The fact that the interaction is local or that the form factors, masses and other dimensional characteristics of particles are nonessential, naturally leads to the conclusion about scale invariance of the hadron interaction cross sections. Scale invariance is one of the characteristic features of cumulative effect.

Over the past years, the cumulative effect has extensively been discussed on the basis of quark-parton models and QCD. In QCD the hypothesis about locality of hadron interaction and a relatively weak coupling of quarks in hadrons are naturally explained by the small value of the running coupling constant and the idea about asymptotic freedom of quarks. The quark-parton model, which is an analog of impulse approximation in nuclear physics, utilizes these fundamental properties of quark matter so as to express the hadron interaction cross

section for elementary interaction of a parton b , being a constituent of hadron B and in terms of the momentum distribution function $G_{B/b}(x, p_{\perp}^2)$ of parton b in hadron B . Here p_{\perp}^2 is the squared transverse momentum of the parton and x is the fraction of the longitudinal momentum of hadron B which is carried by parton b . In particular, the deep inelastic lepton-hadron cross section is of the form

$$\sigma_B(x, Q^2) = \sum_b \sigma_0^b \cdot G_{B/b}(x, Q^2), \quad (1)$$

where σ_0^b is, in the case of electron or muon scattering, the point-like charge interaction cross section, $\sigma_0^b = \frac{A_b}{Q^4}$, $Q^2 = -q^2$ the squared four-momentum transfer, and $x = \frac{Q^2}{2(Pq)}$ is the fraction of momentum p of hadron B which is carried by constituent b . The distribution functions $G_{B/b}(x, Q^2)$ are given the name of quark-parton structure functions. Theory is at present unable to predict them, however, they have a universal character and can be used to express various processes involving hadrons B . As applied to nuclei, it is advisable to introduce quark-parton structure functions of nuclei. In this case, instead of the momentum of the whole nucleus P we introduce a momentum per nucleon $P^0 = P/A$, where A is the atomic weight, and respectively, $x^0 = xA = \frac{Q^2}{2(P^0q)}$. According to the above con-

siderations the cumulative effect is defined as inclusive reactions in the region $x^0 > 1$. The quark-parton structure function of nuclei in this region is the probability that a constituent (quark) carries the momentum of a nucleon group.

Thus, the quark-parton structure functions of nuclei are independent (irreducible to one-nucleon) characteristics* which are the major objects of experimental studies in the domain of relativistic nuclear physics and which are to be explained by modern quark theory.

The above considerations show that the most direct method of measuring quark-parton structure functions of nuclei is the measurement of deep inelastic scattering of leptons on nuclei. However, because of small values of electromagnetic and weak interaction cross sections, the basic information on quark-parton structure functions of nuclei has been extracted from nuclear limiting fragmentation studies^{/2/}. Moreover, the

* An attempt to obtain quark-parton structure functions of nuclei on the basis of the collective tube model has been made by Dar and his co-workers^{/25/}.

data on limiting fragmentation of nuclei have been used to predict^{/7/} the cross section behaviour for deep inelastic muon scattering in the region $x^0 > 1$.

Undetermined but universal quantities entering the cross section for limiting fragmentation of nuclei (contrary to the case of deep inelastic lepton scattering) are the cross section for elementary interaction of constituents and the probability functions for hadronization of a quark to a hadron C , $D_{C/C}(z)$, where z is the fraction of the quark momentum which is carried by hadron C . Starting from the idea of soft color neutralization (hadronization) of partons, one usually assumes that the momentum distribution of produced particles (in the hard spectrum part) practically coincides with the momentum distribution of the partons out of which the particles are produced.

For small transverse momenta of produced particles, the parton elementary interaction cross section can be approximated by a constant. It thus follows that the one-particle inclusive cross section in the cumulative region

$$E \frac{d\sigma}{d\vec{p}} = f(\epsilon, \vec{p}_{\perp}) \quad (2)$$

is proportional to the quark-parton structure function of nuclei. These considerations have just been used to measure the important characteristics of the structure functions. Here

$$\epsilon = \frac{(P_I \cdot P_{II})}{m_I m_{II}} = \text{ch}(y_I - y_{II})$$

is the invariant specific energy of nuclear collision; P_I and P_{II} , the four-momenta of colliding nuclei; y_I and y_{II} , their rapidities; m_I and m_{II} , their masses. In the frame of reference where, e.g., nucleus II is at rest

$$\epsilon = \frac{E_I}{m_I} = \frac{E_I^0}{m_0}, \quad m_0 = 0.931 \text{ GeV}$$

is the atomic mass unit. Thus, in the frame of reference, where one of the colliding nuclei is at rest, ϵ coincides with the energy per nucleon of the incident nucleus in atomic mass units. The colliding nuclei are here considered in a symmetric way. The limiting fragmentation of nuclei corresponds to independence of f of ϵ . If the radius of short-range correlations in rapidity space is assumed to be equal to $\Delta y \approx 2$, then the limiting fragmentation should begin at energies $\epsilon = \text{ch}(y_I - y_{II}) = \text{ch}2 \approx 3.7$ or at relativistic energies of 3.5 GeV/nucleon^{/1/}. Experiment seems to prove this prediction.

In the present paper we have used the cross sections as a function of the variable X which differs from the Bjorken variable X by the account of mass corrections. We obtain an

expression for the variable X for the reaction



To this end, we write the conservation law starting from the hypothesis on minimal missing mass and neglecting the relative motion momenta of partons in I and II

$$(P_I + X \frac{P_{II}}{A} - P_1)^2 = (M_I + X \frac{M_{II}}{A} + m_2)^2 \quad (3)$$

for pions $m_2=0$, for K^- mesons $m_2=m_K$ and so on. Then we have

$$X = \frac{(P_I \cdot P_1) + M_I m_2 + \frac{m_2^2 - m_1^2}{2}}{(P_I \cdot P_{II}) - M_I M_{II} - (P_{II} \cdot P_1) - M_{II} m_2} \quad (4)$$

It is seen from this equation that for deep inelastic scattering of leptons, with the neglect of their masses, X turns into the Bjorken variable.

$$X \approx - \frac{\frac{1}{2}(P_I - P_1)^2}{(P_I \cdot P_{II}) - (P_{II} \cdot P_1)} = - \frac{q^2}{2(P_{II} \cdot q)} = x \quad (5)$$

We recall the main hitherto known facts on nuclear reactions with large momentum transfers (large p_\perp and X).

1. Experimental data on the production cross sections for cumulative particles (π, K, p and so on), that is, for particles with $X > 1$ in the region of limiting fragmentation of nuclei are described by a unique exponential dependence.

2. This property of the cross sections is universal for various nuclei. The parameter

$$\langle X \rangle^{-1} = - \frac{d}{dX} (\ln E \frac{d\sigma}{dp})$$

describing the spectra of various sort cumulative particles is found to be approximately the same. The ϵ dependence of $\langle X \rangle^{-1}$ becomes asymptotic for $\epsilon \geq 3 \div 4$ according to limiting fragmentation of nuclei. The fact that the parameter $\langle X \rangle^{-1}$ is universal, means that the longitudinal distribution of quarks in nuclei is also universal. The above considerations show that this property is the one of the quark-parton structure function of nuclear matter. The latter fact is proved by direct measurement of the quark-parton structure function of nucleus ^{12}C in the reaction $\mu + ^{12}C \rightarrow \mu' + \dots$ with large momentum transfers up to 200 GeV^2/c^2 (see below).

3. The total interaction cross sections for relativistic nuclei, the cross sections for soft processes and the multiple particle production cross sections have the characteristic dependence on the atomic number of nuclei $A^{2/3}$. However the cross sections for cumulative particle production and the production cross sections for particles with large p_\perp^2 , possess the so-called anomalous or enhanced A dependences which are parametrized by power functions of the form A^n , where $n \geq 1$. In this case n turns out to be a function of both X and p_\perp^2 . In the papers of our group it has been shown that parametrization of the cross sections by the A^n dependence is insufficient. It changes with increasing A transforming to a dependence $\sigma \propto A$ for cumulative pions starting with $A \geq 20$ and for cumulative protons starting with $A \geq 100$. In order to make these facts more precise, we had to study limiting fragmentation of a large set of nuclei, which was just the goal of the experimental programme presented below.

4. By the beginning of the experiments mentioned, the p_\perp^2 dependence of the cumulative particle production cross section was not practically studied.

All the above facts were found to be unexpected and could not be explained on the basis of the presently available models. They show that the study of particle production in the region of limiting fragmentation of nuclei and at large momentum transfers, yields essentially new information about the processes which are to be described by means of QCD.

The aim of the present paper is to summarize the results of experimental study of the mentioned regularities and report on new improved data on cumulative production of positive and negative kaons, antiprotons as well as data on cumulative effect in the region $p_\perp \neq 0$.

EXPERIMENTAL DATA

The experiment was performed on a slow extracted beam of the JINR Synchrophasotron. Fig.1 shows the layout of a spectrometer DISK, a detailed description of which is given in ref.^{14/}

In the present paper we give new experimental data on cumulative particle production, as well as summarize previous data from earlier JINR Communications^{11,12,13,14,15/}. The values of inclusive particle production cross sections are given in Tables I-VII where the notation is as follows: θ is the particle emission angle in degrees; p. the particle momentum in MeV/c, for the sake of simplicity the invariant cross sections

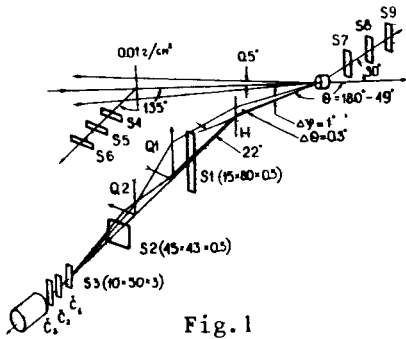


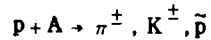
Fig. 1

$$\frac{1}{A} \frac{E}{p^2} \frac{d^2\sigma}{dp d\Omega}$$

are expressed in terms of $d\sigma(\pi^\pm)$ and so on. The cross sections are given in $[\text{mb} \cdot \text{GeV}(\text{GeV}/c)^3 \text{sr}^{-1}]$ per one nucleon of a fragmenting nucleus. The absolute values of the cross sections are measured to within a 15% accuracy.

A. Proton-Nucleus Interactions

Tables I-IV give the cross sections of the reaction



for primary protons with a momentum of 8.9 GeV/c (or $\epsilon = 9.540$). Table I presents energy dependences for Pb, Al, He and D nuclei at 90° and 168° . Such a choice is explained by the aim to obtain experimental information on cumulative particle production for small (168°) and large (90°) values of the transverse momentum. The nuclei chosen, enable us to study the behaviour of the exponent as a function of the atomic number A^n , to within a maximum accuracy for pion production.

Table II presents the estimates of the cross sections for antiproton production in pA interactions in the collision kinematic region of a primary proton with an equivalent target at rest of two or more nucleons. The main source of background processes imitating antiprotons is the registration of protons by a detector adjusted for registration of negative particles. We notice that the ratio of yields of antiprotons and protons is 10^{-6} . However this source of background cannot give a great deal, which is justified by the following fact: when the detector is adjusted for positive particles the deuteron and proton yields are comparable, while for negative particle adjustment antideuterons had not been observed.

Table III gives experimental data on the inclusive cross sections as a function of the atomic weight of a fragmenting nucleus. These data were obtained with the aim to study thoroughly enhanced A dependences. The detailed measurements are seen to be performed for a pion momentum of 500 MeV/c and at 180° (the minimum possible mass of the target at rest is about 1.3 nucleon masses). The set of variables (500 MeV/c, 90°)

and (167 MeV/c, 168°) corresponds to approximately identical minimal target masses, but to essentially different meson momenta, for equal cross sections of interaction of produced mesons with the nucleus.

Experimental data on the angular dependence of the positive pion production cross sections are given in Table IV. The momentum is 500 MeV/c. The angle range from 50° - 180° is necessary for the study of the cross sections as a function of the transverse component of the cumulative particle momentum.

B. Deuteron-Nucleus Interactions

In Tables V-VII we give the cross sections for the reaction



for primary deuterons with a momentum of 8.9 GeV/c (or with $\epsilon = 4.85$). Table V presents data on energy dependence of the pion and kaon production for Pb, Cu and Al nuclei. Table VI presents data on inclusive production cross sections for positive pions ($\times 10^3$) and kaons ($\times 10^4$) at 700 MeV/c as a function of the emission angle ranging from 90° to 180° . Table VII yields data for separated isotopes.

The measurements are seen to be performed by analogy with proton-nucleus interactions so that there is a possibility of studying the dependence of the cross sections on the energy per nucleon of colliding nuclei.

DATA ANALYSIS

A. Energy Spectra

In Fig. 2 we gave experimental data on inclusive pion production cross sections normalized to one nucleon of a fragmenting nucleus as a function of the pion kinetic energy. The solid curves plotted by eye are the experimental data at 90° : the symbols (∇) are the cross sections for dA interaction (divided by 2), (\bullet) those for pA interaction at 8.9 GeV/c for the Pb nucleus and (Δ) at 400 GeV/c for the Ta nucleus^{9/}. The dashed curves are analogous quantities at 168° (160° for 400 GeV). The symbols (\times) show the Institute of Theoretical and Experimental Physics' data at 8.5 GeV/c (160°)^{8/}.

It follows from this figure that:

a) The cross sections are approximately described by exponential functions of the form

$$\exp(-T/T_0). \quad (6)$$

b) The experimental values of the present paper (168°) at 8.9 GeV/c and those of the ITEP group at 8.5 GeV/c coincide to within experimental errors.

c) The cross sections measured in the present paper in the kinetic energy range of mesons up to 1100 MeV change by about 9 orders of magnitude. In this case the minimum value of the invariant cross section corresponds to a few nonabarns.

d) For any energies of produced pions the cross sections are observed to increase with increasing energy per nucleon of interacting nuclei.

e) At low energies ($T < 500$ MeV) of produced mesons, the parameter T_0 in eq. (6) is practically independent of the primary energy (even possibly of the emission angle too), whereas at high energies, especially when comparing our data with those at 400 GeV, the parameter T_0 depends on both the primary energy and emission angle.

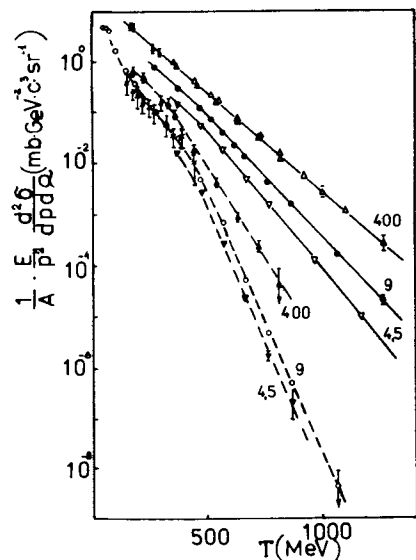


Fig.2

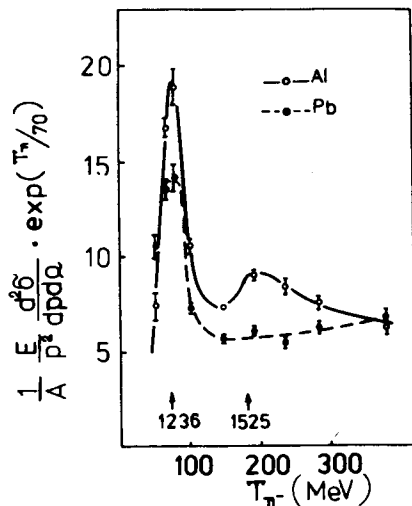
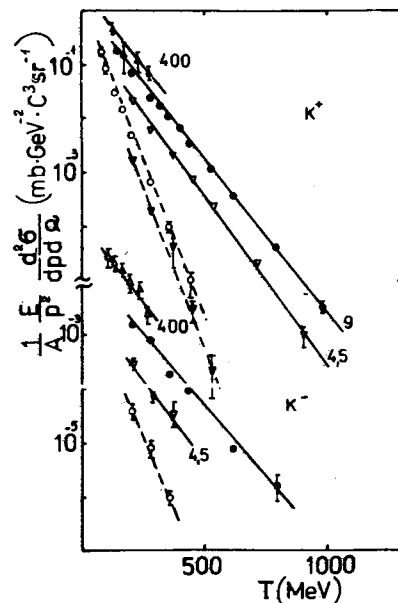


Fig.3

f) At 8.9 GeV primary energy and 168° the pion energy spectrum essentially deviates from the simple exponential dependence (6) at low energies of produced pions. Fig.3 gives these data multiplied by $\exp(T/70)$ for lead and aluminium (Table I). In the energy range from 50–250 MeV the structure is seen to be more sharply peaked for aluminium. The arrows indicate the energies of pions resulting from backward decay of the corresponding binary reaction isobars moving in the direction of the primary proton.



$$\frac{1}{A} \cdot E_p^3 \cdot \frac{d^2 \sigma}{dp^3 d\Omega} \text{ (mb GeV}^2 \text{ c}^3 \text{ sr}^{-1}\text{)}$$

Fig.4

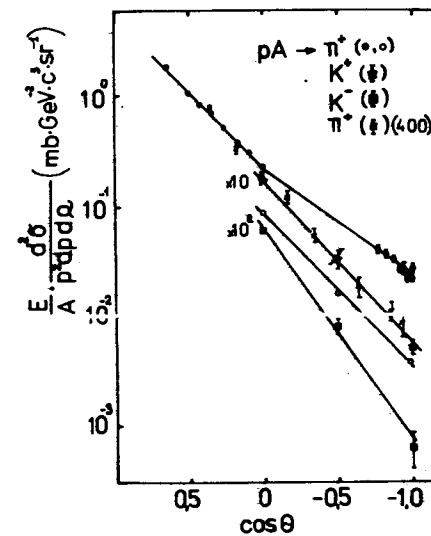


Fig.5

Fig.4 shows experimental data for K^+ (top figure) and K^- (bottom figure) mesons. Again the solid curves correspond to 90° and the dashed ones to 168°. The notation is the same as in Fig.2.

It is seen from Fig.4 that:

a) The K meson production cross sections strongly depend on the primary energy especially for negative kaons.

b) The kaon energy dependence has a smoother exponential behaviour compared to pion data.

Thus, the presentation of all the experimental data in terms of the parametrization (6) shows that the latter is unable to reflect in a satisfactory manner the essential characteristics of cumulative effect: limiting fragmentation and universality of the slope parameter of the energy spectrum. Below it will be shown that the cross section parametrization on the basis of the variable X does not suffer from these shortcomings.

B. Angular Dependences

In Fig.5 we give the experimental inclusive cross sections of production of pions and kaons versus the cosine of the emission angle, for a lead nucleus at 8.9 GeV/c proton momentum (Table I). By the symbols (•) we mark the data for π^+ meson production at 500 MeV/c and by (o) at 600 MeV/c; (*) are the data on 600 MeV/c K^+ mesons increased by a factor of 10; (■) the data on 600 MeV/c K^- mesons increased by a factor of 10^2 . The data on angular dependence for 680 MeV/c π^+ mesons at 400 GeV primary energy^{19/} are given here for comparison.

Fig.6 shows the experimental inclusive cross sections of production of pions (•) and kaons (*) with 700 MeV/c momentum for a lead nucleus bombarded by 8.9 GeV/c deuterons. The angular dependences are seen to be similar.

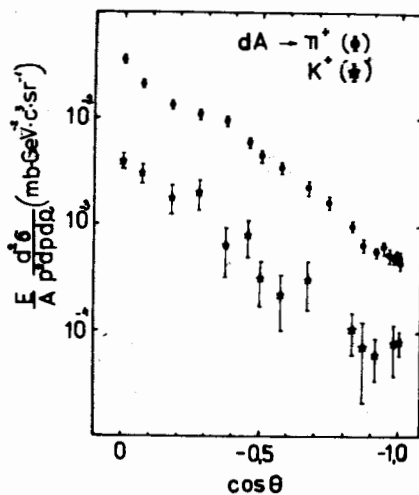


Fig.6

C. Enhanced A Dependence

The cross sections for inelastic interactions of relativistic particles and nuclei with nuclei, are known to possess a characteristic dependence on the atomic number of the type $\sigma \propto A^{2/3}$. There is a natural geometric explanation for this dependence: the cross section is determined by transverse dimensions of an opaque object. An

enhanced (compared to the $A^{2/3}$) dependence was first observed in paper^{18/} for cumulative pion production and then when studying $p_{\perp} \geq 2$ GeV/c particle production on nuclei^{17/}. In these papers the cross sections for production of particles with large momentum transfers were approximated by A^n type dependences and n was observed to reach values larger than unity. The fact that the exponent n may depend on both X and p_{\perp} was already noticed in the first cumulative effect models. It follows from these models that the A dependence is approximate and, generally speaking, insufficient. The discovery of A dependences essentially differing from the simple $A^{2/3}$ dependence was one of the most important signals which pointed out that in the range of large momentum transfers we deal with a new and interesting physics. It should be noted that anomalous or enhanced A dependences are observed when studying effects with small cross sections. The overwhelming majority of the particle-nucleus and nucleus-nucleus interaction cross sections is due to soft processes. These are just the cross sections that possess the characteristic $A^{2/3}$ dependence. For multiple particle production process, in hadronic collisions the transverse momenta are known to be limited and their average values are $\langle p_{\perp} \rangle \sim 0.3 \div 0.4$ GeV/c. Of about the same order of magnitude are the momenta of the nucleon Fermi motion in nuclei. Hence, it follows that soft processes are expected to be well described on the basis of the models in which the nucleons are good quasiparticles. In particular, this is just the reason for which the additive model, where screening effects are taken into account and the nucleus is thought of as a set of nucleons, well explains the behaviour of the cross sections for nucleus-nucleus collisions.

It is very significant that anomalous or enhanced A dependence begins to manifest in the momentum transfer range in which the nucleons, as quasiparticles, lose their importance and nuclear matter should be considered at a quark level. It follows from QCD that such momentum transfers are $Q^2 \gg \Lambda^2$, where Q^2 is the squared four-momentum transfer and $\Lambda \leq 200$ MeV, a characteristic parameter of QCD, that is, for a momentum transfer of 1 GeV/c appropriate quasiparticles are the quarks. With increasing X and p_{\perp}^2 the nucleus must become more opaque since the quark-quark interaction cross section sharply decreases with increasing momentum transfers. On the basis of these suggestions the enhanced A dependence is expected to have the following behaviour: $\sigma \propto A^1$. In other words, the extensively discussed in literature the cross section dependences of the type A^n , where $n > 1$, are not realistic. They were extracted from the study of a small number of nuclei and ac-

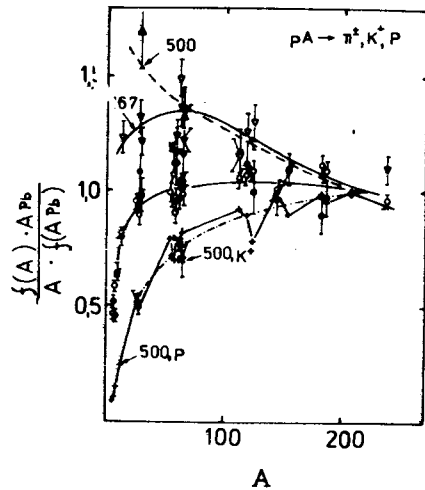


Fig.7

500 MeV/c, the emission angles are 168° and 180° , respectively. The pion production cross sections are seen to sharply increase firstly with increasing A, but starting with $A \sim 20 \div 30$ they remain, within errors, approximately constant per one nucleon of a fragmenting nucleus. Fig.7 (symbols o and •) illustrates the accuracy of experimental data and gives grounds for the conclusion about the behaviour of the enhanced A dependence. It is also seen that the cross sections for the light nuclei (Li, Be) are essentially smaller than the average values. This is, first of all, manifestation of the cluster structure of nuclei.

For positive pions (Table I), we have obtained the following value for the cross section ratio^{15/4}

$$\frac{f({}^6\text{Li} \rightarrow \pi^+) - f({}^4\text{He} \rightarrow \pi^+)}{f(\text{D} \rightarrow \pi^+)} = 2.16 \pm 0.47.$$

As is seen from Tables I-VII, the ratio of the production cross sections for positive and negative pions is close to unity for both pA and dA interactions, that is, for a momentum per nucleon of colliding nuclei larger than 4.2 GeV/c. At lower energies an excess of π^+ mesons compared to π^- mesons is observed, which was studied in detail in the paper by Schroeder et al^{18/}

tually reflect the transition from the $\sigma \propto A^{2/3}$ dependence to the $\sigma \propto A^1$ dependence. We have drawn this conclusion from the study of limiting fragmentation of more than 20 different nuclei and measurement of the cross sections for cumulative particle production in a wide A range.

Fig.7 shows the data taken from Table III. The symbols (o) is the A dependence of the cross sections per nucleon for production of negative pions on a nucleus with atomic weight A, normalized to the cross section per nucleon for the Pb nucleus, as a function of A. For comparison (•) are the corresponding values for positive pions. The pion momentum is

In Table VII we give experimental data for $d\text{Li}^6$ and $d\text{C}^{12}$ interactions resulting in π^+ and π^- meson production:

$$\frac{f(\text{Li} \rightarrow \pi^+) - f(\text{Li} \rightarrow \pi^-)}{f(\text{Li} \rightarrow \pi^+) + f(\text{Li} \rightarrow \pi^-)} = 0.01 \pm 0.05,$$

$$\frac{f(\text{C} \rightarrow \pi^+) - f(\text{C} \rightarrow \pi^-)}{f(\text{C} \rightarrow \pi^+) + f(\text{C} \rightarrow \pi^-)} = 0.03 \pm 0.03.$$

The above-discussed detailed data on the A dependence of the cross sections for cumulative pions with momentum, 500 MeV/c at 180° , corresponds to a cumulative number $X \approx 1.3$. In the same figure triangles are the data for the pion cumulative number $X \approx 0.5$, but for different angles and pion momenta (167 MeV/c , 168°) and (500 MeV/c , 90°). In the case $X \approx 0.5$ the A dependence is seen to have the usual form for soft processes

$$f = E \frac{d\sigma}{d\vec{p}} \propto A^{2/3}. \quad (7)$$

The experimental data on the ratio $\frac{f(A) \cdot A_{\text{Pb}}}{A \cdot f(A_{\text{Pb}})}$ of the production cross sections for 500 MeV/c (180°) pions are shown in the figure by the symbol (+). They are measured to within a 2% accuracy. The behaviour of the A dependence of the cross sections for cumulative protons and pions strongly differs. The cumulative proton production cross sections normalized to A, increase as A increases and a transition to the $f \propto A^1$ dependence appears to proceed only for $A \approx 100$. The dash-dot line is the approximation of the A dependence by the expression

$$f \propto (r_0 A^{1/3} - \rho)^3. \quad (8)$$

Such an approximation follows from the suggestion about finite (nonzero) dimensions of the cumulative proton production region ρ . If this suggestion is valid, then ρ for pions is far less than for protons. Thus, the A^n ($n > 1$) dependences of the cross sections for particle production on nuclei with large momentum transfers, which are widely discussed in literature, are unfounded. They have resulted from an insufficiently thorough study of the mentioned transition of the $f \propto A^{2/3}$ type dependence to the $f \propto A^1$ type dependence. The different behaviour of this transition for various quantum numbers of cumulative particles is seen (Fig.7 symbol (*)) from the experimental data on the production cross sections for K^+ mesons

with 500 MeV/c, at 168° . These data indicate to the difference of the A dependences for pions and kaons and to the similarity for kaons and protons.

The discussed particular features of the A dependences of the cross sections for particle production on nuclei in pA interactions is also observed in dA interactions. In particular, the production cross sections for cumulative pions with $X < 1$ possess the A dependences of the type $f \sim A^{2/3}$, and with $X > 1$, the enhanced A dependences. This is shown in Fig.8 where the data on pion production in dA collisions are plotted. The symbols (Δ) are the data for 600 MeV/c pions at $\theta = 168^\circ$ which corresponds to $X > 1$ and an enhanced A dependence; (∇), the data for $p_\pi = 600$ MeV/c and $\theta_\pi = 90^\circ$; (\bullet), the data for $p_\pi = 215$ MeV/c and $\theta_\pi = 180^\circ$; (σ), the data for $p_\pi = 370$ MeV/c and $\theta = 180^\circ$.

On the basis of the data analysis, we may conclude that the behaviour of the A dependence of the cross sections for production of fast particles on nuclei into the backward hemisphere is determined by the cumulative number, rather than the angle or momentum.

To illustrate this conclusion, as well as to establish an agreement with the earlier experimental data it is advisable to introduce the quantity

$$n = \frac{\ln \frac{f(A_1)}{f(A_2)}}{\ln A_1/A_2} \quad (9)$$

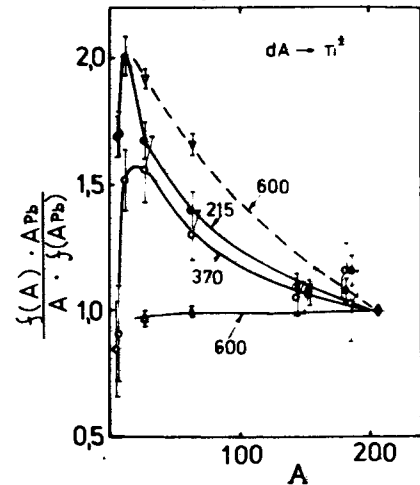


Fig.8

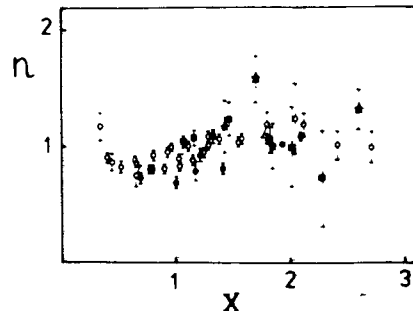


Fig.9

As was shown earlier^{/16/}, n grows from 2/3 to 1, as X changes from 0.4 to 1, and the enhanced A dependence is a characteristic feature of cumulative effect. The experimental data on

$$n' = \frac{\ln f(A_{Pb})/f(A_{Al})}{\ln A_{Pb}/A_{Al}} \quad (10)$$

as a function of the cumulative number X for all pA and dA interactions are given in Fig.9: (\bullet) are the data on pion production in pA interactions; (σ), data on pion production in dA interactions; (\square), the data on K^- mesons. In the same figure the symbols (\star) are the data on K^+ meson production on Pb and Cu nuclei. For $X > 1$, $n=1$ within errors and is independent of X. A rise of n in the range $X < 0.5$ is due to irregular behaviour of the cross sections shown in Fig.3. We notice that a similar dependence was observed in the ITEP experiment^{/20/} and in ref.^{/21/}.

D. Structure Functions of Nuclei

As far as different nuclei are essentially different hadrons, then their limiting nuclei fragmentation cross sections, and correspondingly the quark-parton functions, might be expected to be different. However, as was shown above, these cross sections are rather similar and, being normalized to a simple A dependence, essentially coincide. This enables us to suppose that the quark-parton structure functions of nuclei possess

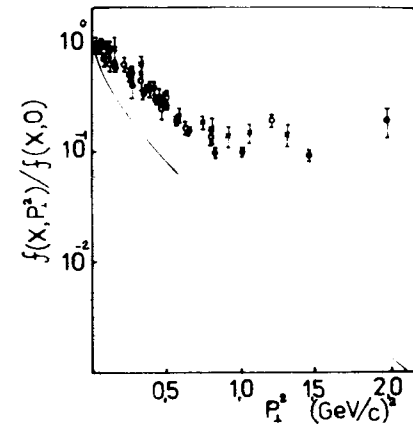


Fig.10

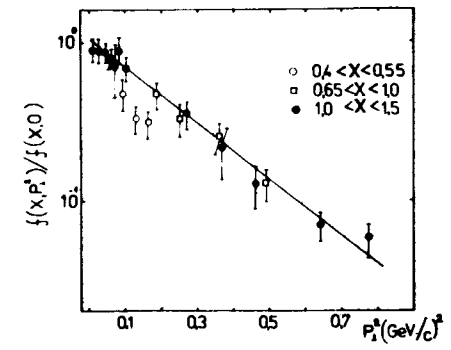


Fig.11

universal properties. Among these properties the dependences of the cross sections on the longitudinal momentum component, or on the cumulative number, are best studied to date.

The experimental data obtained in the present paper enable us to study the cumulative particle production cross section as a function not only of X , but also of p_{\perp}^2 .

Fig.10 shows the ratio of the cross sections of pion production on a lead nucleus for identical X , but different p_{\perp}^2 . The symbols (\bullet) denote the data of the present paper on pA interactions and (\circ) on dA interactions; (\times) are the data on pA interactions at an energy of 400 GeV.

The data on the quantity

$$\phi(p_{\perp}^2) = \frac{f(x, p_{\perp}^2)}{f(x, 0)} \quad (11)$$

given in Fig.10, which belong to different reactions and different energy ranges can be described by a unique function of the form

$$\phi(p_{\perp}^2) = 0.9 \exp(-2.7 p_{\perp}^2) + 0.1. \quad (12)$$

The solid curve shows a similar dependence for the noncumulative region²⁵. We have interpreted the X dependence of the cross section as a longitudinal distribution of partons in nuclei. A similar interpretation of the p_{\perp}^2 dependence of the cross section is invalid because it contains, in addition to the p_{\perp}^2 dependence of the quark-parton function, the p_{\perp}^2 dependence of the parton interaction cross section.

In Fig.11 the cross section of production of cumulative pions on a He nucleus (Table I) is plotted as a function of the transverse momentum. By dividing the experimental values of the cross sections by the function $\phi(p_{\perp}^2)$ (eq. (12)) we obtain the $f(X,0)$ function of the variable X alone. Fig.12 shows

the quantity $G(X) = \frac{1}{A} \cdot \frac{1}{\phi(p_{\perp}^2)} \cdot f(X, p_{\perp}^2)$ obtained in such a way as

for $f(X, p_{\perp}^2)$ we have taken a half of the dA interaction cross section value. The symbols (\bullet) denote $G(x)$ for π^+ mesons, (\star) for K^+ mesons and (\blacksquare) for K^- mesons. In Fig.13 the function $G(X)$ is shown for the pA interaction, for an invariant specific energy $\epsilon = 9.54$.

The following conclusions may be drawn on the basis of Figs.12 and 13:

a) The experimental π^{\pm} and K^+ production cross sections are described to within errors by a unique function $G(X)$.

b) The functions $G(X)$ for π^+ and K^+ mesons are about the same.

c) The function $G(X)$ for K^- is similar to the $G(X)$'s for pions and K^+ mesons but in its absolute value accounts for 5% of the latter.

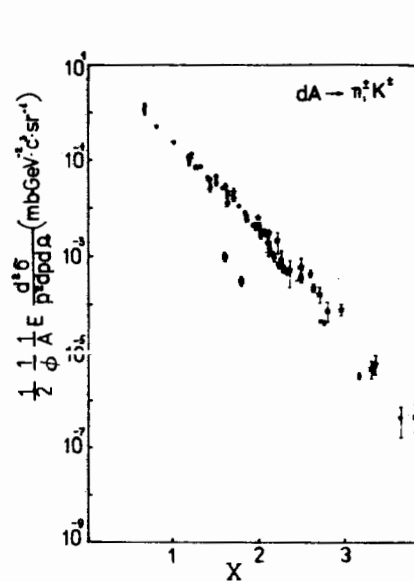


Fig.12

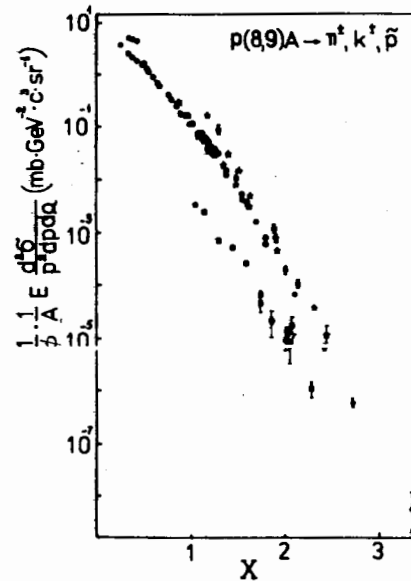


Fig.13

These conclusions are in satisfactory agreement with the quark mechanism predictions for cumulative processes: the valence quarks of colliding objects form a part of the K^+ and π^+ mesons, but do not enter the K^- mesons. The equality of the cross sections for cumulative π^+ and K^+ mesons should be interpreted as a result of pickup from the symmetric quark sea of \bar{d} and \bar{s} quarks by knocked out valence u quarks.

As is shown in ref.¹⁷, the consideration of G(X) as a quark-parton structure function of the nucleus makes it possible to predict the results of experiments on deep inelastic scattering of leptons on nuclei for $X > 1$.

The parametrization of the structure function by the expression of the type

$$G(X) = G_0 \cdot \exp\left[-\frac{X}{\langle X \rangle}\right] \quad (13)$$

makes it possible to extract the parameter $\langle X \rangle$ characterizing the first momentum of the structure function. It is found to be identical for different inclusive reactions¹³, independent of ϵ in a wide energy range $9 \leq \epsilon \leq 400$ and equal to

$$\langle X \rangle \approx 0.14.$$

This parametrization enabled us to predict the results of measurements of the cross sections for deep inelastic scattering of muons on a carbon nucleus at an energy of 280 GeV and large ($Q^2 \approx 100$ (GeV/c)²) momentum transfers²⁷. Thus, the direct measurement of the quark-parton structure function of the nucleus in the reaction $\mu + {}^{12}\text{C} \rightarrow \mu + \dots$ has completely confirmed our interpretation of the cumulative particle production cross sections.

The main result of our investigations is as follows. We have found that a large set of experimental data on cumulative production of pions and kaons can be described by the universal function of the scale invariant variable X, that is, by the quark-parton structure function (13) identical for various nuclei. In the range of the variable

$$0.35 \leq X \leq 3.5$$

examined in the present paper this function changes by 9 orders of magnitudes.

In studying the deep inelastic lepton-nucleus scattering one usually restricts oneself to a range $X < 0.7$. As is seen from the above-said, in the range $X > 0.7$ the nuclear structure function has the simple form (13) and contains less uncertainties than the proton structure function. It can thus be used in deriving the evolution equations for the structure function of the nucleus as the hadron, as well as in verifying QCD working in a far broader range of X than before.

The authors are grateful to Perevozchikov V.G. and Kul'pina O.Yu. for their assistance during the course of this work and the help in the preparation of the manuscript.

TABLE I

θ	P	Li		He	
		$d\delta(\pi^+)$	$d\delta(\pi^-)$	$d\delta(\pi^+)$	$d\delta(\pi^-)$
90°	300			6,34±0,34	
	350			3,01±0,16	2,72±0,14
	400			1,88±0,11	1,54±0,10
	500			(6,63±0,48)10 ⁻¹	(5,08±0,28)10 ⁻¹
	600	(1,70±0,10)10 ⁻¹		(2,22±0,13)10 ⁻¹	(1,75±0,11)10 ⁻¹
	700	(5,15±0,30)10 ⁻²			(3,90±0,33)10 ⁻²
	800			(1,49±0,11)10 ⁻²	(1,27±0,11)10 ⁻²
880			(2,83±0,35)10 ⁻³		
104°	700	(1,39±0,27)10 ⁻²		(1,36±0,30)10 ⁻²	
120°	500	(1,15±0,10)10 ⁻¹		(1,16±0,10)10 ⁻¹	
	600	(1,83±0,15)10 ⁻¹		(2,15±0,24)10 ⁻¹	
	700			(2,58±0,80)10 ⁻³	
154°	500			(3,10±0,68)10 ⁻²	
	600	(4,03±1,37)10 ⁻³		(3,53±1,28)10 ⁻³	
	700	(5,70±2,85)10 ⁻⁴			
162°	500			(2,73±0,28)10 ⁻²	
	600	(2,95±0,58)10 ⁻³			
168°	300			(9,53±0,48)10 ⁻¹	
	350			(3,98±0,23)10 ⁻¹	
	400			(1,53±0,10)10 ⁻¹	
	500			(2,18±0,16)10 ⁻²	
	700			(1,05±0,73)10 ⁻⁴	
180°	150			11,83±0,88	
	175			8,96±0,67	
	200			5,57±0,25	5,05±0,32
	225			3,50±0,20	
	250			2,05±0,12	1,91±0,14
	275			1,26±0,07	
	300			(8,88±0,58)10 ⁻¹	(8,03±0,65)10 ⁻¹
	325			(6,75±0,38)10 ⁻¹	
	350			(4,03±0,35)10 ⁻¹	
	400			(2,03±0,16)10 ⁻¹	(1,95±0,18)10 ⁻¹
	450			(6,63±0,48)10 ⁻²	
500	(1,90±0,14)10 ⁻²		(2,18±0,10)10 ⁻²	(2,53±0,25)10 ⁻²	

TABLE I

		Li		He	
θ	P	$d\delta(\pi^+)$	$d\delta(\pi^-)$	$d\delta(\pi^+)$	$d\delta(\pi^-)$
180°	550			$(7,98 \pm 0,58) 10^{-3}$	
	600			$(2,93 \pm 0,38) 10^{-3}$	$(2,29 \pm 0,65) 10^{-3}$
	650			$(6,85 \pm 0,68) 10^{-4}$	
	700			$(1,59 \pm 0,20) 10^{-4}$	

		D		H	
θ	P	$d\delta(\pi^+)$	$d\delta(\pi^-)$	$d\delta(\pi^+)$	$d\delta(\pi^-)$
90°	500	$(7,25 \pm 0,45) 10^{-1}$			
120°	500	$(5,75 \pm 0,60) 10^{-2}$			
	600	$(5,50 \pm 0,90) 10^{-3}$			
154°	500	$(7,85 \pm 2,1) 10^{-3}$			
180°	150	$9,46 \pm 0,82$		$14,26 \pm 1,52$	
	175	$6,34 \pm 0,35$		$11,36 \pm 0,76$	
	200	$4,16 \pm 0,17$	$3,07 \pm 0,25$	$5,96 \pm 0,38$	$1,78 \pm 0,32$
	225	$2,62 \pm 0,11$		$2,99 \pm 0,24$	
	250	$1,62 \pm 0,08$	$1,51 \pm 0,06$	$2,23 \pm 0,15$	$16,48 \pm 1,06) 10^{-1}$
	275	$1,07 \pm 0,05$		$1,44 \pm 0,12$	
	300	$(7,70 \pm 0,40) 10^{-1}$	$(7,15 \pm 0,50) 10^{-1}$	$1,16 \pm 0,10$	$(2,13 \pm 0,30) 10^{-1}$
	325	$(5,30 \pm 0,30) 10^{-1}$		$(9,70 \pm 0,76) 10^{-1}$	
	340			$(5,48 \pm 0,44) 10^{-1}$	
	350	$(3,05 \pm 0,25) 10^{-1}$		$(3,79 \pm 0,29) 10^{-1}$	
	360			$(2,35 \pm 0,26) 10^{-1}$	
	370			$(1,91 \pm 0,27) 10^{-1}$	
	400	$(7,65 \pm 0,55) 10^{-2}$	$(6,65 \pm 0,65) 10^{-2}$		
	450	$(1,88 \pm 0,12) 10^{-2}$			
	500	$(5,35 \pm 0,55) 10^{-3}$	$(6,25 \pm 1,20) 10^{-3}$		
	550	$(1,32 \pm 0,20) 10^{-3}$			
	600	$(3,3 \pm 3,1) 10^{-4}$	$(4,70 \pm 3,6) 10^{-4}$		
650	$(1,54 \pm 0,43) 10^{-4}$				

TABLE I

		Al			
θ	P	$d\delta(\pi^+)$	$d\delta(\pi^-)$	$d\delta(k^+)$	$d\delta(k^-)$
90°	158		$17,9 \pm 1,7$		
	300		$2,22 \pm 0,03$		
	500	$0,562 \pm 0,06$	$0,345 \pm 0,014$	$(4,4 \pm 0,4) 10^{-2}$	$(1,42 \pm 0,04) 10^{-3}$
	600	$(1,46 \pm 0,03) 10^{-1}$	$(1,23 \pm 0,04) 10^{-1}$	$(1,24 \pm 0,07) 10^{-2}$	$(7,7 \pm 0,4) 10^{-4}$
	700	$(4,93 \pm 0,09) 10^{-2}$	$(4,05 \pm 0,05) 10^{-2}$	$(4,4 \pm 0,7) 10^{-3}$	$(1,57 \pm 0,1) 10^{-4}$
	800	$(1,3 \pm 0,03) 10^{-2}$	$(1,03 \pm 0,03) 10^{-2}$	$(1,64 \pm 0,21) 10^{-3}$	$(6,1 \pm 0,9) 10^{-5}$
	900	$(5,0 \pm 0,06) 10^{-3}$		$(5,9 \pm 0,3) 10^{-4}$	
	1000	$(1,50 \pm 0,07) 10^{-3}$		$(1,86 \pm 0,37) 10^{-4}$	
	1200	$(1,07 \pm 0,1) 10^{-4}$	$(0,89 \pm 0,33) 10^{-4}$	$(1,3 \pm 0,4) 10^{-5}$	$(3,7 \pm 2,5) 10^{-7}$
	1400	$(1,21 \pm 0,22) 10^{-5}$		$(2,1 \pm 0,9) 10^{-6}$	
104°	600	$(0,66 \pm 0,02) 10^{-1}$		$(6,1 \pm 1,4) 10^{-2}$	
120°	600	$(2,3 \pm 0,05) 10^{-2}$		$(2,0 \pm 0,37) 10^{-3}$	
	800	$(0,93 \pm 0,06) 10^{-3}$		$(1,06 \pm 0,16) 10^{-4}$	
168°	125		$3,75 \pm 0,36$		
	152		$6,35 \pm 0,2$		
	167		$6,10 \pm 0,31$		
	200		$2,36 \pm 0,1$		
	250		$0,905 \pm 0,03$		
	300	$0,622 \pm 0,13$	$0,58 \pm 0,03$	$(5,6 \pm 2) 10^{-2}$	
	350	$0,335 \pm 0,10$	$0,27 \pm 0,014$	$(3,2 \pm 0,9) 10^{-2}$	
	400	$(1,65 \pm 0,04) 10^{-1}$	$(1,32 \pm 0,06) 10^{-1}$	$(0,9 \pm 0,16) 10^{-2}$	
	450	$(0,815 \pm 0,02) 10^{-1}$		$(4,7 \pm 1) 10^{-3}$	
	500	$(3,27 \pm 0,1) 10^{-2}$	$(2,71 \pm 0,12) 10^{-2}$	$(2,3 \pm 0,21) 10^{-3}$	
	600	$(4,97 \pm 0,14) 10^{-3}$	$(3,6 \pm 0,06) 10^{-3}$	$(4,5 \pm 0,8) 10^{-4}$	$(0,88 \pm 0,4) 10^{-5}$
	700	$(6,7 \pm 0,7) 10^{-4}$	$(5,3 \pm 0,1) 10^{-4}$	$(4,3 \pm 0,9) 10^{-5}$	$(1,9 \pm 0,55) 10^{-6}$
800		$(4,2 \pm 0,34) 10^{-5}$			
900		$(4,9 \pm 0,6) 10^{-6}$			
1000		$(5,3 \pm 0,7) 10^{-7}$			
1200		$(0,7 \pm 0,7) 10^{-8}$			

TABLE I
Pb

θ	P	$d\delta(\pi^+)$	$d\delta(\pi^-)$	$d\delta(K^+)$	$d\delta(K^-)$
90°	400	0,86 ± 0,02		0,18 ± 0,014	
	500	0,33 ± 0,03	0,32 ± 0,005	7,0 ± 0,3) 10 ⁻²	(1,55 ± 0,06) 10 ⁻³
	600	(1,25 ± 0,03) 10 ⁻¹	(1,26 ± 0,04) 10 ⁻¹	(2,5 ± 0,14) 10 ⁻²	(8,9 ± 0,4) 10 ⁻⁴
	650	(7,7 ± 0,14) 10 ⁻²		(1,82 ± 0,14) 10 ⁻²	
	700	(4,5 ± 0,09) 10 ⁻²	(4,1 ± 0,07) 10 ⁻²	(1,10 ± 0,04) 10 ⁻²	(1,9 ± 0,09) 10 ⁻⁴
	750	(2,43 ± 0,03) 10 ⁻²		(6,65 ± 0,45) 10 ⁻³	
	800	(1,42 ± 0,03) 10 ⁻²		(3,6 ± 0,14) 10 ⁻³	(1,0 ± 0,08) 10 ⁻⁴
	900	(4,4 ± 0,13) 10 ⁻³		(1,19 ± 0,11) 10 ⁻³	
	1000	(1,7 ± 0,04) 10 ⁻³	(1,46 ± 0,06) 10 ⁻³	(3,70 ± 0,3) 10 ⁻⁴	(0,81 ± 0,3) 10 ⁻⁵
	1200	(1,57 ± 0,06) 10 ⁻⁴		(4,7 ± 0,4) 10 ⁻⁵	(1,7 ± 0,9) 10 ⁻⁶
1400	(2,0 ± 0,3) 10 ⁻⁵		(3,6 ± 0,7) 10 ⁻⁶		
120°	600	(2,32 ± 0,44) 10 ⁻²		(4,78 ± 0,9) 10 ⁻³	(1,16 ± 0,2) 10 ⁻⁴
	800	(1,09 ± 0,11) 10 ⁻³		(3,0 ± 0,57) 10 ⁻⁴	(3,4 ± 1,6) 10 ⁻⁶
168°	125		(5,35 ± 0,31)		
	152		(5,15 ± 0,19)		
	167		(4,60 ± 0,26)		
	200		(1,63 ± 0,06)		
	250		0,70 ± 0,03		
	300	0,415 ± 0,01	0,394 ± 0,014	(1,63 ± 0,23) 10 ⁻¹	
	350		0,186 ± 0,01	(0,88 ± 0,16) 10 ⁻¹	
	400	(1,17 ± 0,03) 10 ⁻¹	(1,08 ± 0,06) 10 ⁻¹	(3,0 ± 0,36) 10 ⁻²	
	450	(6,42 ± 0,13) 10 ⁻²		(1,42 ± 0,17) 10 ⁻²	
	500	(3,37 ± 0,09) 10 ⁻²	(2,97 ± 0,11) 10 ⁻²	(5,0 ± 0,4) 10 ⁻³	(4,3 ± 1,4) 10 ⁻⁵
	600	(5,3 ± 0,14) 10 ⁻³	(3,9 ± 0,05) 10 ⁻³	(7,4 ± 1) 10 ⁻⁴	(0,86 ± 0,24) 10 ⁻⁵
	700	(7,57 ± 0,4) 10 ⁻⁴	(6,1 ± 0,09) 10 ⁻⁴	(1,04 ± 0,17) 10 ⁻⁴	(1,04 ± 0,3) 10 ⁻⁶
	800	(5,9 ± 0,45) 10 ⁻⁵	(6,1 ± 0,45) 10 ⁻⁵	(1,04 ± 0,5) 10 ⁻⁵	
	900		(5,1 ± 0,57) 10 ⁻⁶		
1000		(5,2 ± 0,65) 10 ⁻⁷			
1200		(0,47 ± 0,47) 10 ⁻⁸			

TABLE II

θ	P	$d\delta(Pb \rightarrow \bar{p})$	$d\delta(Al \rightarrow \bar{p})$
90°	500	(0,93 ± 0,6) 10 ⁻⁵	(0,85 ± 0,6) 10 ⁻⁵
	700	(2,0 ± 1,2) 10 ⁻⁶	(2,0 ± 1,4) 10 ⁻⁶

TABLE III

$d\delta(A)/d\delta(Pb)$

	π^+ 500, 180°	π^- 500, 168°	π^- 167, 168°	π^+ 500, 90°	K^+ 500, 90°
⁶ Li	0,518 ± 0,032	0,465 ± 0,02			
⁷ Li	0,458 ± 0,03	0,585 ± 0,02			
Be	0,645 ± 0,04	0,629 ± 0,024			
C	0,80 ± 0,04	0,812 ± 0,03	1,23 ± 0,07		
Mg		0,957 ± 0,04			
Al	1,08 ± 0,13	0,894 ± 0,04	1,32 ± 0,07	1,70 ± 0,17	0,51 ± 0,05
Si	0,968 ± 0,08	0,97 ± 0,04	1,21 ± 0,06		
⁵⁴ Fe		0,995 ± 0,04			
⁵⁶ Fe	1,12 ± 0,09	1,07 ± 0,04			
⁵⁸ Fe	1,17 ± 0,1	0,905 ± 0,04			
⁵⁸ Ni	1,12 ± 0,11	0,97 ± 0,04	1,24 ± 0,07		
⁶¹ Ni		0,965 ± 0,04	1,49 ± 0,08		
⁶⁴ Ni	1,16 ± 0,1	1,04 ± 0,05	1,36 ± 0,09		
Cu	1,01 ± 0,08	1,04 ± 0,02	1,36 ± 0,08	1,32 ± 0,05	0,705 ± 0,08
⁶⁴ Zn		0,985 ± 0,04	1,22 ± 0,05		
¹¹² Sn	1,17 ± 0,1	1,06 ± 0,04	1,16 ± 0,07		
¹¹⁸ Sn	1,12 ± 0,1	1,07 ± 0,04	1,26 ± 0,08		
¹²⁴ Sn	1,00 ± 0,1	1,09 ± 0,04	1,30 ± 0,08		
¹⁴⁴ Sm	0,97 ± 0,07	1,01 ± 0,04			
¹⁵⁴ Sm	1,09 ± 0,07	1,09 ± 0,03			
¹⁸² W	0,90 ± 0,08	1,12 ± 0,04			
¹⁸⁶ W	0,975 ± 0,08	1,09 ± 0,04			
Pb	1,00 ± 0,03	1,00 ± 0,02	1,00 ± 0,06	1,00 ± 0,09	1,00 ± 0,04
²³⁸ U		0,956 ± 0,03	1,10 ± 0,06		

TABLE IV
 $\rho = 500$

θ	$\cos \theta$	$d\delta (\pi^+)$
50	0,643	$2,61 \pm 0,09$
60	0,50	$1,53 \pm 0,04$
65	0,422	$1,19 \pm 0,04$
70	0,342	$1,02 \pm 0,04$
75	0,259	$0,74 \pm 0,03$
80	0,174	$0,54 \pm 0,025$
85	0,087	$0,447 \pm 0,023$
90	0	$0,33 \pm 0,03$
I40	-0,766	$(5,85 \pm 0,48) 10^{-2}$
I45	-0,819	$(5,23 \pm 0,44) 10^{-2}$
I50	-0,866	$(4,68 \pm 0,23) 10^{-2}$
I55	-0,907	$(3,75 \pm 0,2) 10^{-2}$
I60	-0,940	$(3,79 \pm 0,39) 10^{-2}$
I65	-0,966	$(3,11 \pm 0,23) 10^{-2}$
I68	-0,978	$(3,37 \pm 0,09) 10^{-2}$
I72	-0,9903	$(3,31 \pm 0,2) 10^{-2}$
I73	-0,9925	$(3,06 \pm 0,2) 10^{-2}$
I74	-0,9945	$(2,74 \pm 0,34) 10^{-2}$
I75	-0,9962	$(2,88 \pm 0,34) 10^{-2}$
I76	-0,9977	$(3,25 \pm 0,38) 10^{-2}$
I77	-0,9986	$(3,02 \pm 0,34) 10^{-2}$
I78	-0,9994	$(3,50 \pm 0,34) 10^{-2}$
I79	-0,9998	$(3,90 \pm 0,34) 10^{-2}$
I80	-1,00	$(3,90 \pm 0,34) 10^{-2}$

TABLE V

P_b

θ	P	$d\delta (\pi^+)$	$d\delta (\pi^-)$	$d\delta (K^+)$	$d\delta (K^-)$
90°	500	$0,268 \pm 0,02$	$0,283 \pm 0,01$	$(3,8 \pm 0,3) 10^{-2}$	$(5 \pm 1) 10^{-4}$
	600	$(0,99 \pm 0,03) 10^{-1}$	$(1,1 \pm 0,03) 10^{-1}$	$(1,03 \pm 0,1) 10^{-2}$	$(1,2 \pm 0,25) 10^{-4}$
	700	$(3,5 \pm 0,14) 10^{-2}$	$(3,6 \pm 0,08) 10^{-2}$	$(3,9 \pm 0,5) 10^{-3}$	$(6,1 \pm 3) 10^{-5}$
	800	$(0,85 \pm 0,08) 10^{-2}$		$(1,5 \pm 0,15) 10^{-3}$	
	900	$(2,98 \pm 0,05) 10^{-3}$		$(4,4 \pm 0,5) 10^{-4}$	
	1100	$(2,33 \pm 0,1) 10^{-4}$		$(4,1 \pm 0,5) 10^{-5}$	
	1300	$(1,66 \pm 0,18) 10^{-5}$		$(1,8 \pm 0,8) 10^{-6}$	
120°	500	$(0,96 \pm 0,02) 10^{-1}$		$(1,40 \pm 0,2) 10^{-2}$	
	600	$(2,45 \pm 0,07) 10^{-2}$		$(2,2 \pm 0,3) 10^{-3}$	
	700	$(4,4 \pm 0,5) 10^{-3}$		$(3,1 \pm 1,4) 10^{-4}$	
	800	$(8,3 \pm 0,3) 10^{-4}$		$(1,3 \pm 0,2) 10^{-4}$	
168°	500	$(2,50 \pm 0,1) 10^{-2}$		$(3,2 \pm 0,5) 10^{-3}$	
	600	$(4,47 \pm 0,14) 10^{-3}$	$(4,35 \pm 0,17) 10^{-3}$	$(3,7 \pm 0,8) 10^{-4}$	
	700	$(4,92 \pm 0,3) 10^{-4}$	$(5,6 \pm 0,3) 10^{-4}$	$(7,7 \pm 3,9) 10^{-5}$	
	800	$(4,4 \pm 0,4) 10^{-5}$	$(4,3 \pm 0,7) 10^{-5}$	$(5,5 \pm 2,3) 10^{-6}$	
	900	$(3,1 \pm 0,5) 10^{-6}$		$(4,3 \pm 3,2) 10^{-7}$	
	1000		$(4,1 \pm 2,5) 10^{-7}$		
180°	215	$1,51 \pm 0,11$	$1,14 \pm 0,1$		
	372	$0,11 \pm 0,02$	$0,1 \pm 0,02$		
	700	$(4,4 \pm 0,4) 10^{-4}$		$(8 \pm 2) 10^{-5}$	

TABLE V

Cu

θ	ρ	$d\delta(\pi^+)$	$d\delta(\pi^-)$	$d\delta(\pi^+)$
90°	600	0,163 ± 0,005		(0,85 ± 0,24) 10 ⁻²
	800	(1,4 ± 0,03) 10 ⁻²		(1,6 ± 0,17) 10 ⁻³
120°	600	(2,72 ± 0,07) 10 ⁻²		(1,82 ± 0,3) 10 ⁻³
	800	(1 ± 0,03) 10 ⁻³		(0,91 ± 0,16) 10 ⁻⁴
168°	500	(3,37 ± 0,1) 10 ⁻²		(1,76 ± 0,6) 10 ⁻³
	600	(4,4 ± 0,12) 10 ⁻³		(2,3 ± 0,9) 10 ⁻⁴
180°	215	1,83 ± 0,13	1,9 ± 0,13	
	372	(1,35 ± 0,16) 10 ⁻¹	(1,34 ± 0,15) 10 ⁻¹	
	458		(3,8 ± 0,5) 10 ⁻²	
	546		(0,9 ± 0,1) 10 ⁻²	
	605		(2,8 ± 0,9) 10 ⁻³	

Al

θ	ρ	$d\delta(\pi^+)$	$d\delta(\pi^-)$	$d\delta(\pi^+)$
90°	600	0,189 ± 0,004		(0,78 ± 0,1) 10 ⁻²
	800	(1,26 ± 0,02) 10 ⁻²		(1,6 ± 0,2) 10 ⁻³
120°	600	(2,82 ± 0,06) 10 ⁻²		(1,09 ± 0,14) 10 ⁻³
	800	(0,7 ± 0,03) 10 ⁻³		(2,5 ± 0,8) 10 ⁻⁵
168°	600	(4,3 ± 0,1) 10 ⁻³		(1,4 ± 0,4) 10 ⁻⁴
180°	215	2,14 ± 0,14	2,32 ± 0,12	
	372	(1,6 ± 0,2) 10 ⁻¹	(1,62 ± 0,2) 10 ⁻¹	
	458		(3,9 ± 0,5) 10 ⁻²	
	546		(1 ± 0,2) 10 ⁻²	
	605		(3,5 ± 1,4) 10 ⁻³	

TABLE VI

 $\rho = 700$

θ	$-\cos\theta$	$d\delta(\pi^+) 10^3$	$d\delta(k^+) 10^4$
90°	0	35,3 ± 1,4	39 ± 5
94°	0,07	21,2 ± 1,3	30,5 ± 6
100°	0,174	13,5 ± 1,2	17,6 ± 5
106°	0,2756	10,7 ± 1,2	19,7 ± 6
112°	0,3748	9,3 ± 1,0	6,3 ± 3
117°	0,4537	5,83 ± 0,7	8 ± 3
120°	0,50	4,39 ± 0,5	3,1 ± 1,4
125°	0,5734	3,42 ± 0,4	2,2 ± 1,2
132°	0,6692	2,22 ± 0,3	3,1 ± 1,5
138°	0,7434	1,65 ± 0,22	
146°	0,8290	0,99 ± 0,11	1,05 ± 0,5
150°	0,8660	0,66 ± 0,1	0,72 ± 0,5
156°	0,9136	0,56 ± 0,06	0,6 ± 0,26
160°	0,9397	0,63 ± 0,09	
164°	0,9613	0,54 ± 0,08	
168°	0,9782	0,49 ± 0,03	0,77 ± 0,39
172°	0,9903	0,52 ± 0,05	
177°	0,9967	0,50 ± 0,07	0,6 ± 0,2
180°	1,00	0,44 ± 0,04	

TABLE VII

	$\rho = 215$		$\rho = 372$	
	$d\delta(\pi^+)$	$d\delta(\pi^-)$	$d\delta(\pi^+)$	$d\delta(\pi^-)$
⁶ Li	2,27 ± 0,17	2,23 ± 0,18	0,109 ± 0,03	0,07 ± 0,03
⁷ Li	2,13 ± 0,14	2,40 ± 0,23	0,111 ± 0,03	0,08 ± 0,03
C	2,75 ± 0,15	2,61 ± 0,12	0,172 ± 0,014	0,142 ± 0,01
¹¹⁴ Sm	1,56 ± 0,1	1,37 ± 0,1	0,115 ± 0,012	0,102 ± 0,014
¹⁵⁴ Sm	1,40 ± 0,09	1,46 ± 0,1	0,106 ± 0,012	0,117 ± 0,014
¹⁸² W	1,55 ± 0,1	1,32 ± 0,09	0,12 ± 0,01	
¹⁸⁶ W	1,61 ± 0,1	1,47 ± 0,11	0,107 ± 0,016	

REFERENCES

1. Baldin A.M. Fizika Element. Chastits i Atomm. Yadra, Moskva, Energoizdat, 1977, vol.8, issue 3, p.429.
- Baldin A.M. Proc. of the XIX Int.Conf. on High Energy Physics, Tokyo, 1978, p.455.
2. Stavinsky V.S. Fizika Element. Chastits i Atomm. Yadra, Moskva, Energoizdat, 1979, vol.10, issue 5, p.949.
3. Leksin G.A. Proc. of the XVIII Int.Conf. on High Energy Physics, Tbilisi, 1976.
4. Avericheva T.V. et al. JINR, 1-11317, Dubna, 1978.
5. Baldin A.M. Brief Communications on Physics, Acad. of Sci. of the USSR, 1971, 1.
6. Baldin A.M., Stavinsky V.S. Proc. of the V Intern. Seminar on High Energy Physics Problems, JINR, D1,2-12036, Dubna, 1978, p.261.
7. Baldin A.M. JINR, E1-80-545, Dubna, 1980.
8. Burgov N.A. et al. ITEP - 58, 1979.
9. Nikiforov N.A. et al. Phys.Rev.C, 1980, v.22, N.2, p.700.
10. Baldin A.M. Proc. of the Int. Conf. on Extreme States in Nuclear Systems, Dresden, 1980, v.2, p.1.
11. Baldin A.M. et al. JINR, P1-11302, Dubna, 1978.
12. Baldin A.M. et al. JINR, 1-80-488, Dubna, 1980.
13. Stavinsky V.S. Proc. of the VI Intern. Seminar on High Energy Physics Problems, JINR, D1,2-81-728, Dubna, 1981.
14. Baldin A.M. et al. JINR, P1-11168, Dubna, 1977.
15. Baldin A.M. et al. JINR, 1-82-28, Dubna, 1982.
16. Baldin A.M. et al. Yadernaja Fizika, 1974, vol.20, issue 6.
17. Cronin J.W. et al. Phys.Rev.D., 1975, v.11, p.3105.
18. Schroeder L.S. et al. Phys.Rev.Lett., 1979, v.43, N 24, p.1787.
19. Baldin A.M. et al. Proc. of the IV Intern. Seminar of High Energy Physics Problems, JINR, D1,2-9224, Dubna, 1975, p.176.
20. Bajukov Yu.D. et al. ITEP - 30, 1979.
21. Alanakian K.V. et al. YPI - 455(6) - 80, Yerevan, 1981.
22. Strikman M.I., Frankfurt L.L. Fizika Element. Chastits i Atomm. Yadra, Moskva, Energoizdat, 1980, vol.11, issue 3, p.571.
23. Baldin A.M. et al. Yadernaja Fizika, 1975, vol.21, issue 5.
24. Stavinsky V.S. JINR, P2-80-767, Dubna, 1980.
25. Barlad G. et al. Phys.Rev.D., 1980, v.22, 7, p.1547.
26. Efremov A.V. Yadernaja Fizika, 1976, vol.24, issue 6, p.1208.
27. Savin I.A. Proc. of the VI Intern. Seminar on High Energy Physics Problems, JINR, D1,2-81-728, Dubna, 1981.

Received by Publishing Department
on July 21 1982.

Балдин А.М. и др. Экспериментальные результаты по инклюзивному сечению рассеяния для кумулятивного образования пионов, каонов, антипротонов и кварк-партоновая структурная функция ядра

Статья содержит наиболее полное представление экспериментальных данных по образованию π^{\pm} , K^{\pm} , и \bar{p} в заднюю полусферу в реакциях pA и dA. Представленные в работе энергетические угловые зависимости сечений изображены также в переменных X /обобщение масштабной переменной/ и p_1^2 . Зависимость сечений от X интерпретируется в терминах универсальной кварк-партоновой структурной функции ядра G(X). Область $X > 1$ соответствует кумулятивному эффекту, где структурные функции ядра рассматриваются как самостоятельные /не сводимые к однонуклонным/ объекты адронной физики. Продольное распределение кварков в ядрах G(X) оказалось в пределах ошибок одинаковым для всех ядер: $G(X) \approx \exp[-X/0,14]$. В данной работе оно изучено в интервале $0,25 \leq X \leq 3,4$, где сечение кумулятивного эффекта меняется на 9 порядков величины. Использование большого набора ядер позволило детально изучить так называемые усиленные или аномальные A-зависимости для жестких процессов на ядрах. Показано, что широко обсуждаемые в литературе зависимости типа A^n , где $n > 1$, не обоснованы. При больших A и $X > 1$ зависимости сечений выходят на режим $\sigma \sim A^1$.

Работа выполнена в Лаборатории высоких энергий ОИЯИ.

Сообщение Объединенного института ядерных исследований. Дубна 1982

Baldin A.M. et al. Experimental Data on Inclusive Cross Section for Cumulative Production of Pions, Kaons, Antiprotons and the Quark-Parton Structure Function of Nuclei E1-82-472

The paper is a complete presentation of the experimental data on backward π^{\pm} , K^{\pm} , and \bar{p} production in pA and dA reactions. The energy and angular dependences of the cross sections are also given in terms of X (generalization of the scaling variable) and p_1^2 . The X dependence of the cross sections is interpreted in terms of the universal quark-parton structure function of the nucleus G(X). The region $X > 1$ corresponds to cumulative effect where the nuclear structure functions are considered as independent (irreducible to one-nucleon) objects of hadron physics. The longitudinal distribution of quarks in nuclei G(X) was found to be, to within errors, identical for all the nuclei: $G(X) \approx \exp[-X/0,14]$. In the present paper it was studied in the range $0.25 \leq X \leq 3.4$, where the cumulative production cross section varies by 9 orders of magnitude. The use of a large set of nuclei made it possible to study the so-called enhanced or anomalous A dependences for hard processes on nuclei. The dependences of the type A^n , where $n > 1$, widely discussed in literature are shown to be groundless. For large A and $X > 1$ the dependences depart to the asymptotic region $\sigma \sim A^1$.

The investigation has been performed at the Laboratory of High Energies, JINR.

Communication of the Joint Institute for Nuclear Research. Dubna 1982